Materials and Design 36 (2012) 477–481

Contents lists available at SciVerse ScienceDirect

Materials and Design

journal homepage: www.elsevier.com/locate/matdes

Study on plastic damage of AISI 304 stainless steel induced by ultrasonic impact treatment

Xinjun Yang, Jianxin Zhou, Xiang Ling *

Jiangsu Key Laboratory of Process Enhancement and New Energy Equipment Technology, School of Mechanical and Power Engineering, Nanjing University of Technology, Nanjing 210009, China

ARTICLE INFO

Article history:
Received 8 October 2011
Accepted 10 November 2011
Available online 25 November 2011

Keywords:
C. Surface treatments
A. Ferrous metals and alloys
E. Mechanical

ABSTRACT

The plastic damage of AISI 304 stainless steel induced by the ultrasonic impact treatment has been studied by using finite element model based on Gurson–Tvergaard–Needleman (GTN) ductile damage constitutive equations in this paper. There is a maximum compressive residual stress with −370 MPa when the impact velocity is 5 m/s, and the location of maximum residual compress stress is at the depth of 0.2 mm from the treated surface. Meanwhile, the depth of the compressive residual stress increases from 0.65 mm to 0.85 mm when the impact velocity changes from 3 m/s to 5 m/s. The damage area is annular and the indent center is not affected. The damage depth is only 0.07 mm from the specimen surface. It is reasonable to remove about 0.1 mm thickness material from the treated surface which can not only keep the compressive residual stress and hardened surface but also avoid the surface roughness and plastic damage to material surface.

1. Introduction

The material failure including wear, corrosion and fatigue is dependent on the surface states [1,2], so many surface modification technologies have been used to significantly improve mechanical properties and behaviors of materials. Ultrasonic impact treatment (UIT) is a cold working treatment which forms the surface nanocrystalline and hardening by the surface severe plastic deformation [3–5]. Compared with other methods such as shot peening [1], ultrasonic shot peening [6], surface mechanical attrition [7] and laser shock processing [8,9], UIT is more controllable and convenient to be applied in the industry production.

UIT has been studied from the early 1970s [10]. The principle of UIT is based on the vibration of rod by using high power ultrasound. Because of the high frequency of the system, the treated specimen surface is mechanically peened with a great number of impacts in a short time [11]. To date, UIT has been used to improve the properties of titanium, AISI321 stainless steel and Aluminum (Al) matrix composite. The researchers found that the top surface of the materials can be nanocrystallized and the influence depth of compressive residual stress can reach more than 1 mm. All these increased the fatigue durability of different metallic materials [12]. Both the nanostructure and residual stress were shown to attribute to the essential increase of hardness [13]. It was also found that the microhardness of the Al matrix composite induced by UIT was about 1.1 GPa even after heating to 623 K [14]. UIT is successfully employed to enhance the fatigue life of different welding joints. The compressive residual stress, the refined grain size of the weld joint, and the groove formation in the transition area between the weld seam and parent material had been found to be the main features of UIT promoting the welded joints properties [15–17].

The finite element method provides a powerful method for simulating the single/multiple shots/pins impact on a target. Several models conducted to simulate the impact process by using the finite element method. Some of them were axi-symmetric models to simulate the single shot/pin impact [18]. Others were developed by using three-dimensional finite element models in order to be more realistic [19]. The subjected material behavior law was supposed, in some cases elastic plastic, and in other cases rate-sensitive materials [20,21]. All these simulations allowed predicting the introduced plastic deformation and residual stress profile in the near surface.

UIT is an effective way to enhance the properties of the materials, and the main benefits get from the treatment including surface gain refinement, surface compressive residual stress, and increasing surface hardness. However, the rough surface generated by UIT may mask the beneficial effects of UIT. The collision between the material surface and the pin may also cause the microstructure damage on the material. In this paper, a finite element model based on Gurson–Tvergaard–Needleman (GTN) ductile damage constitutive equations is established to study the plastic damage of AISI 304 stainless steel during UIT [22].

* Corresponding author. Tel.: +86 25 83243112; fax: +86 25 83600956.
E-mail address: Xling@njut.edu.cn (X. Ling).

0261-3069/$ - see front matter © 2011 Elsevier Ltd. All rights reserved.
doi:10.1016/j.matdes.2011.11.023

2. The UIT process

A UIT equipment consists of ultrasonic generator with a frequency of about 21 kHz and an output power of about 1.5 KW, piezo-ceramic transducer, step-like ultrasonic horn made from strength material, and the impact head installed on the horn tip. The impact head contains cylindrical pin(s) which can free move between the horn tip and the treated surface. The schematic diagram of UIT is shown in Fig. 1.

The mechanical energy P per impact [23] can be estimated considering that pins acquire their kinetic energy from the vibrating ultrasonic horn tip (E_{us}) (vibration frequency f_{us} and amplitude ξ) and from the moving of the impact head/sample (E_r). Thus, it is estimated according to the following expression:

$$P(W/g/\text{impact}) = \frac{f_i E_k}{m} = \frac{f_i}{m}(E_{us} + E_r) \approx \frac{f_i}{m}[2\pi^2 f_{us}^2 \xi^2 m_P + E_r] \quad (1)$$

where $f_i \approx 3 \pm 0.5$ kHz is an impacting frequency, m is the coefficient with the mass dimension, which takes into account the correlation between the pin mass m_P and the sample mass m_s. During the treatment, the repeated multidirectional impact at high rates onto specimen surface leads to severe plastic deformation on the surface. The main parameters of the ultrasonic impact treatment process are as follows: the vibration frequency driven by an ultrasonic generator is 20 kHz, the pin's diameter and length are 3 mm and 25 mm, respectively. In this study, the peening velocity changed from 3 mm/s to 5 mm/s, in which the E_r was ignored.

3. Damage model

It is considered that the ductile damage is induced by the evolution of micro-void under local stress–strain field, and it is nearly impossible to observe it experimentally because the time between the growth of void and the last failure of material is too short. The Gurson–Tvergaard–Needleman (GTN) model could simulate the micro-voids nucleation, growth, coalescence effectively. The GTN model is first proposed by Gurson [24], and modified by Tvergaard and Needleman [22], expressed as follows:

$$\frac{\sigma_e^2}{\sigma_y^2} + 2q_1 f^* \cos h\left(q_2 \frac{3\sigma_m}{2\sigma_y}\right) - (1 + q_3 (f^*)^2) = 0 \quad (2)$$

where σ_e is von Mises stress, σ_y is the yield stress of material, σ_m is mean stress, q_1, q_2 and q_3 are the constitutive parameters, f^* is the current effective void volume fraction (VVF), which considers void coalescence phenomenon, in the definition of the yield criterion:

$$f^*(f) = \begin{cases} f & \text{if} \quad f \leqslant f_c \\ f_c + \frac{q_1^{-1} - f_c}{f_F - f_c}(f - f_c) & \text{if} \quad f_c < f < f_F \end{cases} \quad (3)$$

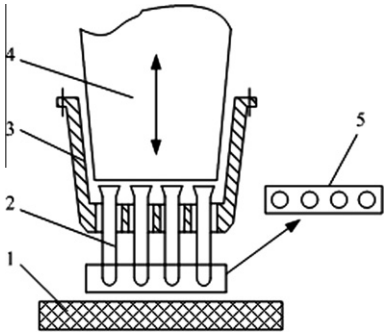

Fig. 1. Impact head used in UIT: (1) sample, (2) pin (s), (3) head body, (4) ultrasonic horn and (5) the array of pins on the head.

where f_c is the critical VVF, referring to the beginning of void coalescence, and f_F is the final failure VVF, that is to say, material will be failure completely when the current VVF equal to f_F.

The evolutional rate of VVF consists of void volume grow rate of existing voids $\dot{f}_{\text{growth}}$, and new nucleation rate $\cdot f_{\text{nucl}}$, that is:

$$\begin{cases} \dot{f} = \dot{f}_{\text{growth}} + \dot{f}_{\text{nucl}} \\ F(t_0) = f_0 \end{cases} \quad (4)$$

where f_0 is initial VVF of intact material, which represents the initial damage induced by slag inclusions.

$\dot{f}_{\text{growth}}$depends on plastic volume strain rate, described as:

$$\dot{f}_{\text{growth}} = (1 - f) \sum^{pl} \quad (5)$$

Nucleation is considered to base exclusively on effective plastic strain and the void nucleation follows normal distribution, characterized as follows:

$$\dot{f}_{\text{nucl}} = \frac{f_N}{S_N \sqrt{2\pi}} \exp\left(-\frac{1}{2}\left(\frac{\varepsilon_M^{pl} - \varepsilon_N}{S_N}\right)\right) \dot{\varepsilon}_M^{pl} \quad (6)$$

where f_N is the maximum volume of micro-particles which have potential to turn into voids through new nucleation in the material, ε_N is the critical mean value of plastic strain referring the beginning of void coalescence, S_N is the corresponding standard deviation, ε_M^{pl} is equivalent plastic strain, and $\dot{\varepsilon}_M^{pl}$ is equivalent plastic strain rate.

According to Franklin formula [25], f_0 can be determined from the amount of chemical composition of sulfur and manganese in the tested material:

$$f_0 \approx 0.054\left(\text{S}(\%) - \frac{0.001}{\text{Mn}(\%)}\right) \quad (7)$$

f_c could be confirmed using the expression proposed by Benseddiq [26]:

$$f_c = 0.0186\ \text{Ln}(f_0) + 0.1508 \quad (8)$$

f_F could be obtained from Zhang's empirical relation between f_0 and f_F [27], which is written as:

$$f_F = 0.15 + 2 \times f_0 \quad (9)$$

The values of q_1, q_2 and q_3 are fixed to 1.5, 1.0 and 2.25 as suggested by Tvergaard and Needleman.

4. Finite elements model

The two-dimensional axi-symmetric FE model was developed using the commercial finite element code ABAQUS Explicit 6.6 to investigate the damage on the materials during UIT for single impact (Fig. 2). As shown in Fig. 2, the target was modeled as a rectangular body (6 mm × 15 mm), which was large enough to avoid the effects of the boundary conditions on the results. The impact area was (2 mm × 2 mm) located in the contact side of the rectangular. Target mesh was set by CAX4R: 4-node bilinear axisymmetric quadrilateral element with reduced integration and hourglass control. The diameter and length of the steel pin were 1.5 mm and 5 mm, respectively. The steel pin was modeled as a rigid whose element was CAX 3-node linear axisymmetric triangle. A sensitivity study had already been carried out to optimize the dimensions of the element in the refine zone. The size of the target was $0.1 \times 0.05\ \text{mm}^2$ and $0.1 \times 0.1\ \text{mm}^2$, and in the contact area was refine into $0.05 \times 0.05\ \text{mm}^2$.

To simplify the damage analysis, AISI304 stainless steel was adopted in this model, and the mechanical properties of AISI304 stainless steel were presented in Fig. 3 (σ_b = 668 MPa, σ_s = 286 MPa,

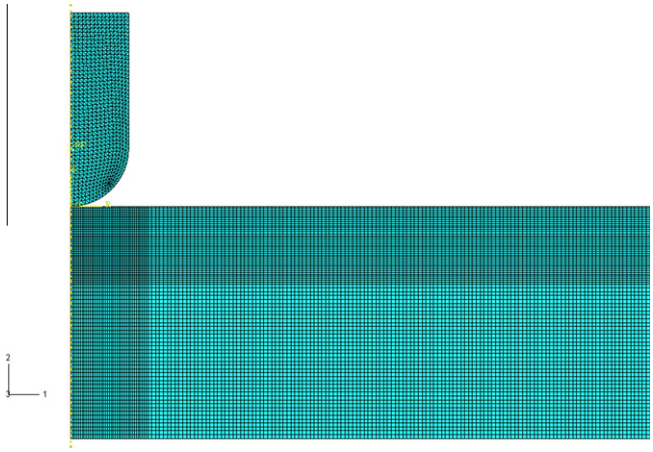

Fig. 2. Finite element model.

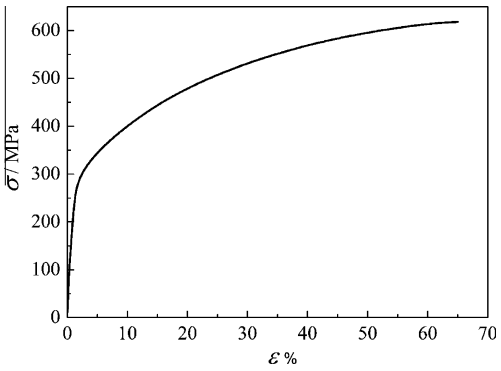

Fig. 3. The σ–ε curve of AISI 304 stainless steel.

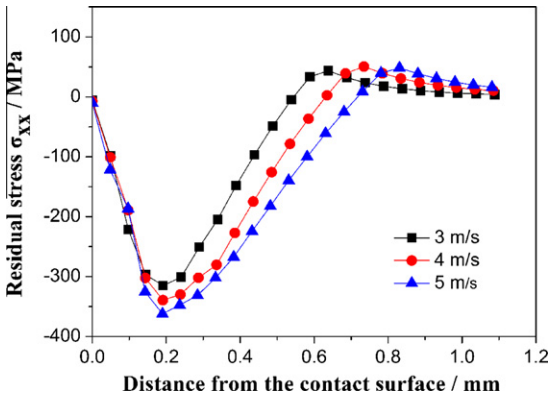

Fig. 4. Residual stress at different impact velocities.

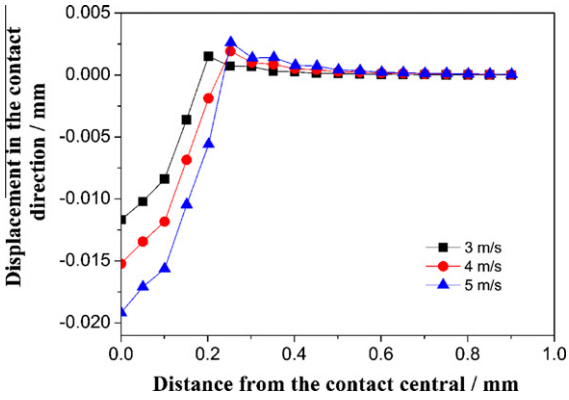

Fig. 5. Displacement for the points on the contact surface at different impact velocities.

υ = 0.3). The parameters of GTN were the same as mentioned in Section 3.

The bottom of the model was restrained against all displacements and rotations. The left was the axial symmetry boundary condition. The impact velocities employed were 3 m/s, 4 m/s and 5 m/s, respectively.

5. Results and discussion

Fig. 4 shows the residual stress distribution obtained by numerical simulation as functions of impact velocity. The maximum compressive residual stresses are all located at the depth of about 0.2 mm from the treated surface at three different impact velocities. The similar results can be seen in Ref. [28], and the reason may be due to the grain refinement of surface layer generated by mechanical effect [29]. The maximum compressive residual stress increases from about −320 MPa to −370 MPa when the impact velocity changes from 3 m/s to 5 m/s. According to the Eq. (1), the injected energy per impact is square of the velocity [23]. For the material hardening induced by UIT, the compressive residual stress sluggishly increases with the impact velocity from 3 m/s to 5 m/s [1]. As the strain-hardening material is used, the maximum compressive residual reached 1.3 σ_s, which is 30% higher than the initial yield stress of the target. Comparing with results of simulation using elastic–plastic model, the maximum compressive residual stress induced by UIT in this study is smaller than in that case [13]. This is because the GTN model used in this paper considering the material containing micro-voids, it breaks the continuity of the material in the elastic–plastic model without damage, and decreases the strength of the material [30]. During the UIT process, this makes the compressive residual stress a little smaller. Meanwhile, the depth of the compressive residual stress also increases from 0.65 mm to 0.85 mm. It can be found from Fig. 4 that the impact velocity has little effect on the locations of maximum compressive residual stress, but it shows significant effect on the maximum compressive residual stress and the depth of the compressive stress zone. The results agree well with the result obtained in Ref. [19] about shot peening.

Fig. 5 is the displacement of the points on the contact surface at different impact velocities. The displacement is 0.012 mm when the impact velocity is 3 mm/s. However, the displacement increases to 0.019 mm at the impact velocity of 5 mm/s. Considering the basic concepts of the various peening method, the surface roughness behavior is evidently due to the random nature of impact of the metallic balls. Comparing with such peening method, like shot peening, the roughness magnitude after UIT in this paper is larger. It is because the impaction of the metallic balls or pins with lateral load can lead to the shallow indent and the broader indent width [12]. For the recovery of the elastic deformation of the material after impaction whose pins without the tangential velocity in the UIT process, the width of the displacement point is nearly invariable at different velocities [13]. Hence, it can be concluded the increasing impact velocity can increase the stress concentration.

The damage evaluation in the process of UIT is presented by using the parameter VVF in this paper. The plastic damages of AISI 304 stainless steel at different impact velocities are shown in Fig. 6a–6c. It can be seen that the plastic damage increases with the increasing impact velocity. According to the GTN equations, nucleation is considered to base exclusively on effective plastic

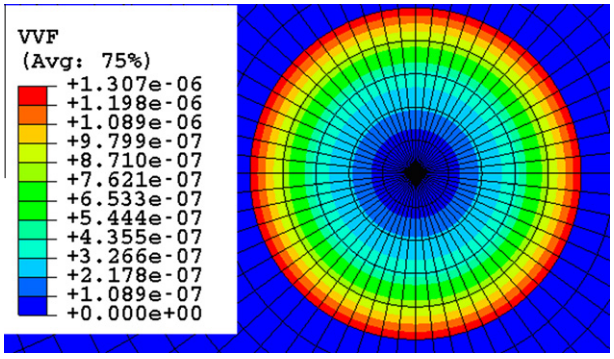

Fig. 6a. The VVF distributions on the treated surface at the impact velocity of 3 mm/s.

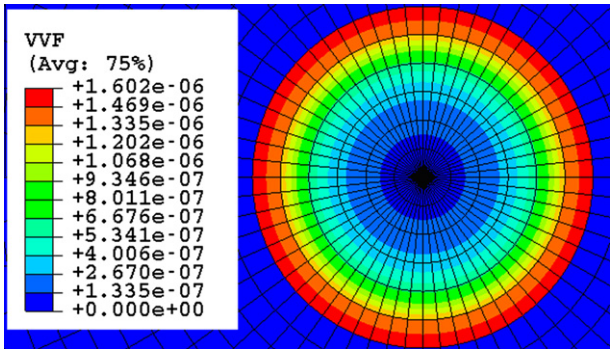

Fig. 6b. The VVF distributions on the treated surface at the impact velocity of 4 mm/s.

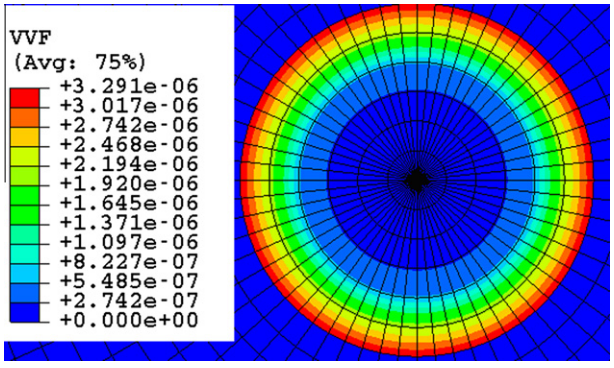

Fig. 6c. The VVF distributions on the treated surface at the impact velocity of 5 mm/s.

strain and the void nucleation follows normal distribution, characterized as Eq. (6). The increase of the impact velocity enhances the equivalent plastic strain ε_M^{pl} and also the equivalent plastic strain rate $\dot{\varepsilon}_M^p$ in the UIT process. Meanwhile, the damage is caused by the tension in the process of UIT. So the damage value VVF increases with the impact velocity [24]. The damage area in the process is annular in which the maximum damage locates in the outboard of impact zone. The indent center is not affected by UIT from the viewpoint of the void growing. The damage depth is only about 0.07 mm from the contact surface, which is shown in Fig. 7. From Figs. 5–7, it is reasonable to remove about 0.1 mm thickness material from the treated surface, which means the compressive residual stress and hardened surface can be kept. In addition, the surface roughness and plastic damage to materials could be avoided.

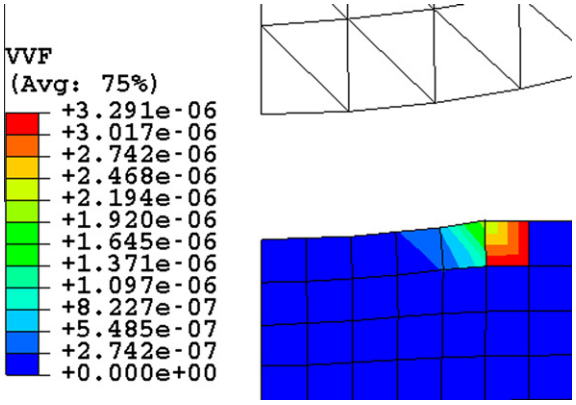

Fig. 7. The VVF distribution along specimen thickness at the impact velocity of 5 mm/s.

6. Conclusions

The plastic damage of AISI 304 stainless steel induced by UIT has been studied by using finite element model based on GTN ductile damage constitutive equations. The results show that the maximum compressive residual stress changes from about −320 MPa to −370 MPa and locates at the depth of 0.2 mm from the treated surface when the impact velocity changes from 3 m/s to 5 m/s. Meanwhile, the depth of the compressive residual stress increases from 0.65 mm to 0.85 mm. The damage area in the process of UIT is annular and the indent center is not affected. The damage depth is only about 0.07 mm from the contact surface. Removal of surface layer with 0.1 mm thickness material from the treated surface is an effective method, which not only keeps the compressive residual stress and hardened surface but also avoids the surface roughness and plastic damage of material surface.

Acknowledgment

The authors wish to acknowledge the financial support provided by the National Natural Science Foundation of China (Grant No. 50875121).

References

[1] Wagner L. Mechanical surface treatments on titanium, aluminum and magnesium alloys. Mater Sci Eng A 1999;263:210–6.
[2] Peters JO, Boyce BL, Chen X, McNaney JM, Hutchinson JW, Ritchie RO. On the application of the Kitagawa–Takahashi diagram to foreign-object damage and high-cycle fatigue. Eng Fract Mech 2002;69:1425–46.
[3] Conrad H, Narayan J. Mechanisms for grain size hardening and softening in Zn. Acta Mater 2002;50:5067–78.
[4] Dinda GP, Rosner H, Wilde G. Synthesis of bulk nanostructured Ni, Ti and Zr by repeated cold-rolling. Scr Mater 2005;52:577–82.
[5] Gleiter H. Nanostructured materials basic concepts and microstructure. Acta Mater 2000;48:1–29.
[6] Lu K, Lu J. Surface nanocrystalline (SNC) of metallic materials-presentation of the concept behind a new approach. J Mater Sci Technol 1999;15:193–7.
[7] Tao NR, Wang ZB, Tong WP, Sui ML, Lu J, Lu K. An investigation of surface nanocrystallization mechanism in Fe induced by surface mechanical attrition treatment. Acta Mater 2002;50:4603–16.
[8] Lu JZ, Luo KY, Zhang YK, Cui CY, Sun GF, Zhou JZ, et al. Grain refinement of LY2 aluminum alloy induced by ultra-high plastic strain during multiple laser shock processing impacts. Acta Mater 2010;58:3984–94.
[9] Lu JZ, Zhong JW, Luo KY, Zhang L, Dai FZ, Chen KM, et al. Micro-structural strengthening mechanism of multiple laser shock processing impacts on AISI 8620 steel. Mater Sci Eng A 2011;528:6128–33.
[10] Statnikov ES, Zhuravlev LV, Alekseev AF, Bobylev YA, Shevtsov EM, Sokolenko VI, Kulikov VF. Ultrasonic head for strain hardening and relaxation treatment (in Russian), USSR Inventor's Certificate No. 472782, Published in Byull. Izobret. No. 21; 1975 (Priority of 1972)
[11] Morgyuk BN, Prokopenko GI. Fatigue life improvement of α-titanium be novel ultrasonically assisted technique. Mater Sci Eng A 2006;437:396–405.

[12] Mordyuk BN, Prokopenko GI. Ultrasonic impact peening for the surface properties' management. J Sound Vib 2007;308:855–66.
[13] Mordyuk BN, Milman YV, Ilefimov MO, Prokopenko GI, Silberschmidt VV, Danylenko MI, et al. Characterization of the ultrasonically peened and laser-shock peened surface layers of AISI321 stainless steel. Surf Coat Technol 2008;202:4875–83.
[14] Mordyuk BN, Ilefimov MO, Prokopenko GI, Golub TV, Danylenko MI, Kotko AV. Structure, microhardness and damping characteristics of Al matrix composite reinforced with AlCuFe or Ti using ultrasonic impact peening. Surf Coat Technol 2010;204:1590–8.
[15] Huo L, Wang D, Zhang Y. Investigation of the fatigue behaviour of the welded joints treated by TIG dressing and ultrasonic peening under variable-amplitude load. Int J Fatigue 2005;27:95–101.
[16] Yin D, Wang D, Jing H, Huo L. The effects of ultrasonic peening treatment on the ultra-long life fatigue behavior of welded joints. Mater Des 2010;31:3299–307.
[17] Zhao X, Wang D, Huo L. Analysis of the S–N curves of welded joints enhanced by ultrasonic peening treatment. Mater Des 2011;32:88–96.
[18] Guagliano M. Relating Almen intensity to residual stresses induced by shot peening: a numerical approach. J Mater Process Technol 2001;110:277–86.
[19] Hong T, Ooi JY, Shaw B. A numerical simulation to relate the shot peening parameters to the induced residual stress. Eng Fail Anal 2008;15:1097–110.
[20] Meguid SA, Shagal G, Sttranart JC. 3D FE analysis of peening of strain-rate sensitive materials using multiple impingement model. Int J Impact Eng 2002;27:119–34.
[21] Frijaa M, Hassineb T, Fathallahc R, Bouraouib C, Doguib A. Laboratoire de Genie Mecanique. Finite element modelling of shot peening process: prediction of the compressive residual stresses, the plastic deformations and the surface integrity. Mater Sci Eng A 2006;426:173–80.
[22] Tvergaard V, Needleman A. Analysis of the cup-cone fracture in a round tensile bar. Acta Metall 1984;32:157–69.
[23] Sekkal AC, Langlade C, Vannes AB. Tribological transformed structure of titanium alloy (TiAl6V4) in surface fatigue induced by repeated impacts. Mater Sci Eng A 2005;393:140–6.
[24] Gurson AL. Continuum theory of ductile rupture by void nucleation and growth: part 1-yield criteria and flow rules for porous ductile materials. J Eng Mater Technol 1977;99:2–15.
[25] Franklin A. Comparison between a quantitative microscope and chemical methods for assessment of non-metallic inclusions. J Iron Steel Inst 1969;207:181–6.
[26] Benseddiq N, Imad A. A ductile fracture analysis using a local damage model. Int J Press Vessels Pip 2008;85:219–27.
[27] Zhang ZL, Thaulow C, Phidegard J. A complete Gurson model approach for ductile fracture. Eng Fract Mech 2000;67:155–68.
[28] Luo KY, Lu JZ, Zhang YK, Zhou JZ, Zhang LF, Dai FZ, et al. Effects of laser shock processing on mechanical properties and micro-structure of ANSI 304 austenitic stainless steel. Mater Sci Eng A 2011;528:4783–8.
[29] Lu JZ, Luo KY, Zhang YK, Sun GF, Gu YY, Zhou JZ, et al. Grain refinement mechanism of multiple laser shock processing impacts on ANSI 304 stainless steel. Acta Mater 2010;58:5354–62.
[30] Lu JZ, Luo KY, Zhang YK, Zhou JZ, Cui XG, Zhang L, et al. Effects of laser shock processing and strain rate on tensile property of LY2 aluminum alloy. Mater Sci Eng A 2010;528:730–5.